



The evolution of coexistence from competition in experimental co-cultures of *Escherichia coli* and *Saccharomyces cerevisiae*

Jake N. Barber¹ · Aysha L. Sezmis¹ · Laura C. Woods¹ · Trenton D. Anderson¹ · Jasmyn M. Voss¹ · Michael J. McDonald¹ 

Received: 20 May 2020 / Revised: 6 October 2020 / Accepted: 7 October 2020 / Published online: 22 October 2020
© The Author(s), under exclusive licence to International Society for Microbial Ecology 2020

Abstract

Microbial communities are comprised of many species that coexist on small spatial scales. This is difficult to explain because many interspecies interactions are competitive, and ecological theory predicts that one species will drive the extinction of another species that competes for the same resource. Conversely, evolutionary theory proposes that natural selection can lead to coexistence by driving competing species to use non-overlapping resources. However, evolutionary escape from extinction may be slow compared to the rate of competitive exclusion. Here, we use experimental co-cultures of *Escherichia coli* and *Saccharomyces cerevisiae* to study the evolution of coexistence in species that compete for resources. We find that while *E. coli* usually outcompetes *S. cerevisiae* in co-culture, a few populations evolved stable coexistence after ~1000 generations of coevolution. We sequenced *S. cerevisiae* and *E. coli* populations, identified multi-hit genes, and engineered alleles from these genes into several genetic backgrounds, finding that some mutations modified interactions between *E. coli* and *S. cerevisiae*. Together, our data demonstrate that coexistence can evolve, de novo, from intense competition between two species with no history of coevolution.

Introduction

Competition between microbial species is probably more common than cooperation [1]. Can two species that compete for the same resource evolve to coexist? Theory predicts that if competition between species is strong, then one species is likely to drive the other extinct [2]. However, there are mechanisms that can promote coexistence—equalising forces that reduce the fitness differences between competing species, and stabilising forces that reduce negative interspecific interactions [3]. Equalising mechanisms act to reduce the rate of competitive exclusion so that, even if species depend on the same resources, they can coexist

neutrally for extended periods [4–6]. Alternatively, stabilising mechanisms promote coexistence by reducing interspecific interactions, for example, by niche differentiation [4, 7]. Recent work has shown that evolutionary and ecological processes act over similar timescales in a process known as eco-evolutionary feedback [8–12]. Evidence for eco-evolutionary feedback has been found in a wide variety of model systems, ranging from laboratory populations of *Bacillus subtilis* [11], *Caenorhabditis elegans* and its parasite *Bacillus thuringiensis* [13], *Drosophila melanogaster* [14], the plant species *Lemna minor* and *Spirodela polyrhiza* [15] and island populations of *Anolis* lizards [12]. The prevalence of eco-evolutionary feedback among these model systems suggest these coexistence mechanisms may be able to evolve in newly formed communities comprised of competing species.

Evolution experiments with populations of microbes have shown that rates of adaptation are sufficient for multiple coexisting ecotypes to evolve from a single progenitor during a laboratory experiment [16–20]. A well characterised example is the evolution of *P. fluorescens* SBW25 in spatially structured microcosms, where intraspecific competition drives the evolution and maintenance of at least two ecotypes [19, 20]. Experimental adaptive radiation has

These authors contributed equally: Jake N. Barber, Aysha L. Sezmis

Supplementary information The online version of this article (<https://doi.org/10.1038/s41396-020-00810-z>) contains supplementary material, which is available to authorized users.

✉ Michael J. McDonald
mike.mcdonald@monash.edu

¹ School of Biological Sciences, Monash University, Monash, VIC, Australia

also been observed in the microbial eukaryote *S. cerevisiae*, which rapidly evolves two, coexisting, ecotypes in non-shaking microwell plates [21]. In both cases, strong intraspecific competition and the availability of alternative niches in heterogenous environments provided the opportunity for the evolution of novel ecotypes.

There is also an evidence of eco-evolutionary feedback mechanisms at work in homogenous environments [12, 15, 22, 23]. In one well-known example, *E. coli* populations propagated in environments with glucose as the sole carbon source can evolve to secrete high levels of acetate, a by-product of fermentation. This acetate waste product can be exploited as a carbon source by a second ecotype that evolves during the experiment [24, 25]. In other experiments with *E. coli*, the loss of the capacity to produce an amino acid was found to be advantageous, as long as there was enough of that amino acid being produced by other *E. coli* cells in the population [26]. Partially engineered microbial models have also been used to study the relationship between consumers and producers of specific metabolites [27–30]. These systems lead to the evolution of mutualisms, as costly excretions can be exploited as a resource when a mutualistic partner can offer something in return [31–33]. Studies of naturally co-occurring bacteria often find the presence of mutualisms that avoid niche overlap in complex systems [1, 34–37]. These studies of multi-species communities provide many insights into coevolution and multi-species interactions, however, since these interspecies interactions are pre-existing, it is difficult to trace the evolutionary origins of coexistence.

Taken together, these evolution experiments have shown that diversification frequently evolves in single species evolution experiments. However, the outcome for two or more evolving species in co-culture is less certain. Theory predicts that coexistence is more likely to evolve when the initial fitness difference between species is small [4, 38], and two ecotypes evolved from the same species are much more likely to have growth rates compatible with coexistence than two competing species. While there have been experimental studies of coevolving species, most have focused on species with established relationships, such as phage and their bacterial hosts [39, 40] or natural and synthetic bacterial communities that already coexist [35, 37, 41]. These, and studies of coevolving bacteria, have found that the presence of multiple species can drastically alter the outcomes of evolution [35]. In this study, we explore the evolutionary origins of coexistence by coculturing two species, a prokaryote (*E. coli*) and a eukaryote (*S. cerevisiae*), within a homogenous environment. These two species have been well characterised and have a suite of genetic and genomic resources. Since these two organisms do not have a history of coexistence in nature [42, 43], and are competitively mismatched in the lab, this

allows us to explore the genetic basis of the eco-evolutionary mechanisms that lead to the *de novo* evolution of coexistence.

Results

E. coli is competitively superior to *S. cerevisiae* in co-culture conditions

To study the evolutionary origins of coexistence, we propagated replicate populations of *E. coli* and *S. cerevisiae* in either monoculture or co-culture treatment conditions. We used a nutrient-rich complex growth medium with glucose (4%) and yeast extract, and incubated cultures with rapid shaking to evenly distribute nutrients and reduce spatial structure (“Methods”). The monoculture treatment consisted of either *S. cerevisiae* or *E. coli* grown in isolation from the other species. In the co-culture treatment, *S. cerevisiae* and *E. coli* were propagated together in the same vessel (Fig. 1A). We tracked the presence of both species in each population to monitor rates of competitive exclusion. In the first phase of the experiment (420 generations, Fig. 1), *E. coli* tended to outcompete *S. cerevisiae*, until only two of the initial 60 replicate co-culture populations contained both species (Fig. 1B). This confirmed that, in the co-culture conditions of this experiment, *E. coli* has a superior competitive fitness to *S. cerevisiae*. For the second phase of the experiment, the two co-culture wells remaining after 420 generations were used to found 60 new replicate co-culture populations (30 each). After these were propagated for a further 560 generations, four of the 60 co-culture populations maintained both *E. coli* and *S. cerevisiae*, while *S. cerevisiae* had fixed in three populations and *E. coli* had fixed in the remaining 53 cultures (Fig. 1C, D). Altogether, the co-culture and monoculture populations were propagated for around 980 generations. Each of the 60 monoculture populations in phase two were founded by transfer directly from the 60 monocultures from phase one (Fig. 1B).

We set up replicate cultures of the four co-cultures (B10, C6, E7, and E10) that remained after 980 generations to determine the new equilibrium frequencies of *E. coli* and *S. cerevisiae*. We tracked the frequencies of *E. coli* and *S. cerevisiae* for 70 generations, to determine whether the two species could persist in co-culture. While *E. coli* had fixed in nearly all ancestral co-cultures ($f_{E. coli} = 0.994$, CI ± 0.005), the evolved co-cultures maintained an equilibrium at around 60% *E. coli* ($f_{E. coli} = 0.58$, CI ± 0.059), significantly different from the equilibrium frequency of the *E. coli* and *S. cerevisiae* ancestors (post-hoc t-test, $p < 1 \times 10^{-4}$) (Fig. 2A). Since the *E. coli* ancestor nearly always outcompeted the *S. cerevisiae* ancestor, these data

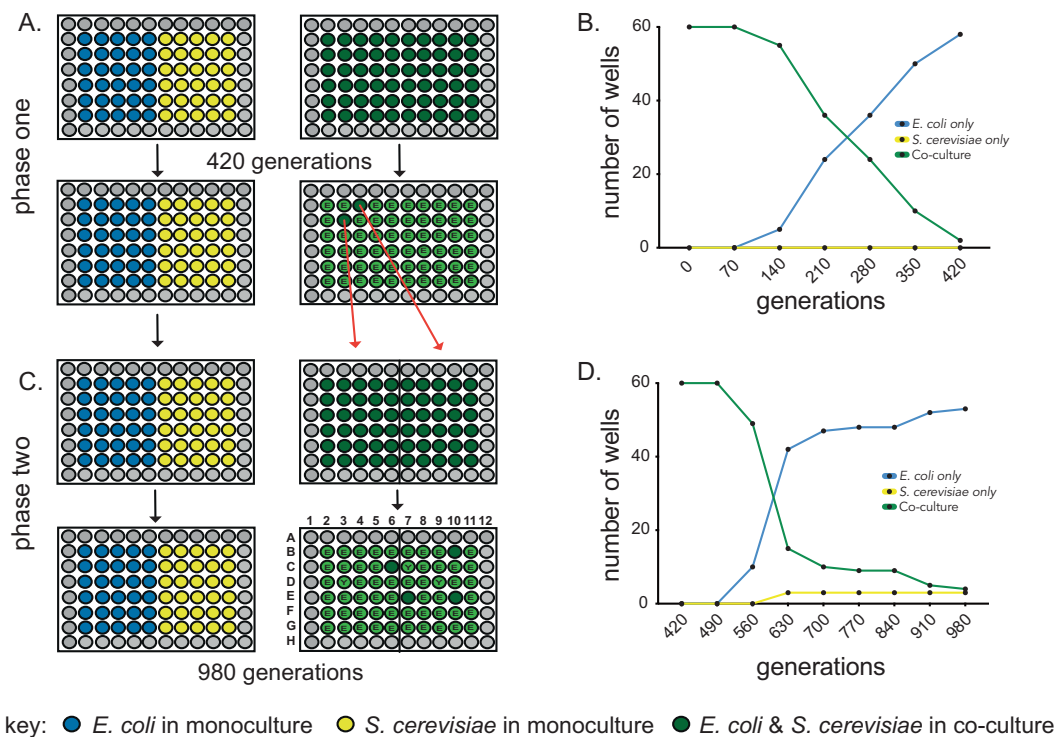


Fig. 1 Experimental co-evolution of *E. coli* and *S. cerevisiae*. **A** Replicate populations of *E. coli* and *S. cerevisiae* were propagated as either monoculture or co-culture for 420 generations (phase one). **B** The species composition of 60 co-culture replicate populations were tracked with *S. cerevisiae* going extinct in 58/60 wells. **C** These two persisting co-cultures were each used to found 30 replicate populations

and propagated for 580 generations (phase two) and **D** the species composition of the co-cultures tracked. Letters inside green circles indicate that either *E. coli* (E) or *S. cerevisiae* (Y) has fixed in that co-culture. Alphanumeric well positions (e.g. "C6") are used to refer to specific populations.

show that the co-culture evolved *E. coli*/*S. cerevisiae* pairs were able to persist in co-culture for significantly longer than the pair of ancestral strains.

The evolution of co-culture specific adaptations in *S. cerevisiae* and *E. coli*

Previous evolution experiments have found that coevolution can speed rates of adaptation. We carried out competition assays between the evolved co-culture populations and their corresponding ancestor. *S. cerevisiae* that evolved in co-culture adapted more rapidly to the growth medium than *S. cerevisiae* that evolved in monoculture (Mann–Whitney test, $p = 1.1 \times 10^{-3}$) (Fig. 2B). Fitness assays showed that while both the winning and co-culture *E. coli* were significantly fitter than the ancestor strain (post-hoc *t*-test, $p < 0.01$), neither were significantly fitter than monoculture *E. coli* (post-hoc *t*-test, $p > 0.05$) (Fig. 2B). These results suggest that only co-cultured *S. cerevisiae* that adapted faster than average had the potential to persist in co-culture with *E. coli*.

Ecologically stable coexistence is defined by the ability of each species to invade from rare. To test whether the

genetic changes that evolved in *S. cerevisiae* were sufficient for *E. coli*/*S. cerevisiae* coexistence, we carried out reciprocal invasion assays of ancestral *E. coli* against evolved and ancestral *S. cerevisiae*. We founded cultures with a range of starting frequencies for each species, ranging between 9:1 and 1:9 (*E. coli*:*S. cerevisiae*) (Fig. 2C, D). We found strong genotype-dependent effects across different combinations of *S. cerevisiae* and *E. coli* regardless of the initial frequency ratios (Fig. 2C, D). Ancestral *E. coli* could form stable co-culture with two of the evolved co-cultured *S. cerevisiae*, B10 and C6, (Fig. 2C) with ancestral *E. coli* comprising around 30–40% of the co-culture. This was lower than the frequency of *E. coli* in evolved co-cultures (50–60% *E. coli*). Conversely, ancestral *S. cerevisiae* was not able to form stable co-culture with any of the co-culture evolved *E. coli* (Fig. 2D). These data show that the evolutionary changes in co-culture evolved *S. cerevisiae* were necessary and sufficient for coexistence with *E. coli*. However, since co-culture evolved *E. coli* attained higher frequencies in co-culture than ancestral *E. coli*, this suggests that there was also further evolutionary changes in co-culture evolved *E. coli*.

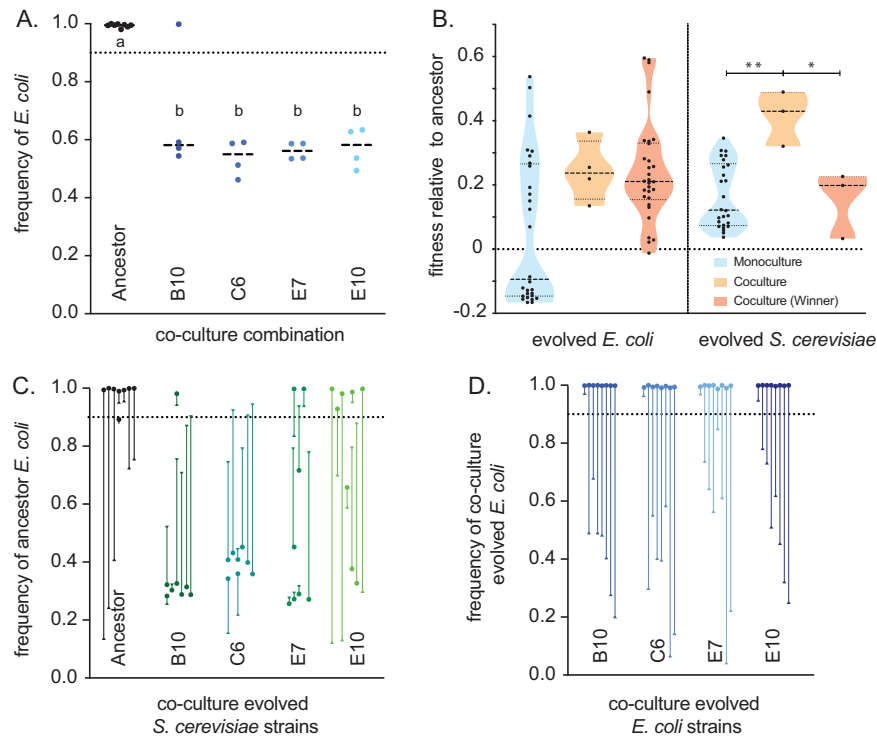


Fig. 2 The evolution of stable *E. coli* - *S. cerevisiae* co-cultures. **A** The equilibrium frequency of *S. cerevisiae* and *E. coli* co-culture for ancestral (black dots) and co-culture evolved strains (coloured dots) expressed as the frequency of *E. coli* ($f_{E. coli}$). **B** The fitness of evolved monoculture populations (blue), populations that persisted in co-culture for 980 generations (orange), and “winners”, populations that outcompeted its opposite species in co-culture during the second phase (generation 420–980) of the evolution experiment. *E. coli* strains are shown in the left panel and *S. cerevisiae* shown on the right panel. Stars show significant differences between individual comparisons

using Bonferroni-corrected Mann–Whitney U tests. **C** The final equilibrium frequency of ancestral *E. coli* co-cultured with ancestor and co-culture evolved *S. cerevisiae* populations after an invasion assay; and **D** ancestral *S. cerevisiae* with co-culture evolved *E. coli*. An equilibrium frequency of “1” means that *E. coli* has driven *S. cerevisiae* extinct, and 0.5 means that *E. coli* and *S. cerevisiae* are equally represented in stable co-culture. Arrows start at the inoculation frequency for each of the replicate populations. Capitalised letters show different groups as designated by Tukey’s post-hoc test.

Parallel evolution suggests co-culture specific adaptation in *E. coli* but not *S. cerevisiae*

To determine the genetic causes of adaptation, we sequenced *S. cerevisiae* and *E. coli* populations taken from monoculture and co-culture treatments (Fig. 3, Supplementary Data file). The evolution of mutations in the same gene or genetic pathway across independent replicate populations is evidence for the action of natural selection. We looked for multi-hit genes, or genes that were mutated across all replicate populations for a given treatment. In *S. cerevisiae*, we identified 146 mutations across 9 sequenced populations. However, no genes stood out as co-culture specific. We identified a single multi-hit gene, BUL1, that had evolved distinct nonsynonymous substitutions in both co-culture and monoculture populations. In *E. coli*, we found a clear delineation between the mutations that fixed in co-culture and those that fixed in monoculture populations (Fig. 3). We identified mutations across all evolved *E. coli* populations (monoculture and co-culture)

that have been described in previous evolution experiments with *E. coli* MG1655. Indel mutations between *pryE* and *rph* known to restore a fitness defect in MG1655 were found in 11 of the 12 populations that we sequenced. Mutations in *spoT* and *nadR* are known to increase fitness in evolution experiments with glucose as the sole carbon source, and fixed in every *E. coli* population. Other mutational differences evolved that were specific to the monoculture and co-culture treatments, respectively (Fig. 3). Each monoculture *E. coli* population that we sequenced had a unique mutation that disrupted the *dusB-fis* operon. Co-culture populations showed parallelism in three genes, *glyQ*, *btuB*, and *fhuA* (Supplementary Data). *glyQ* is an essential gene involved in tRNA synthesis, attaching glycine to its relevant tRNA for subsequent protein construction. Interestingly, *btuB* and *fhuA* are TonB-dependent transmembrane transporters of vitamin B12 (*btuB*) and ferrichrome siderophores (*fhuA*), respectively. Both are also implicated in the uptake of a range of toxins and antibiotics produced by microbes and is a receptor for a range of bacteriophage.

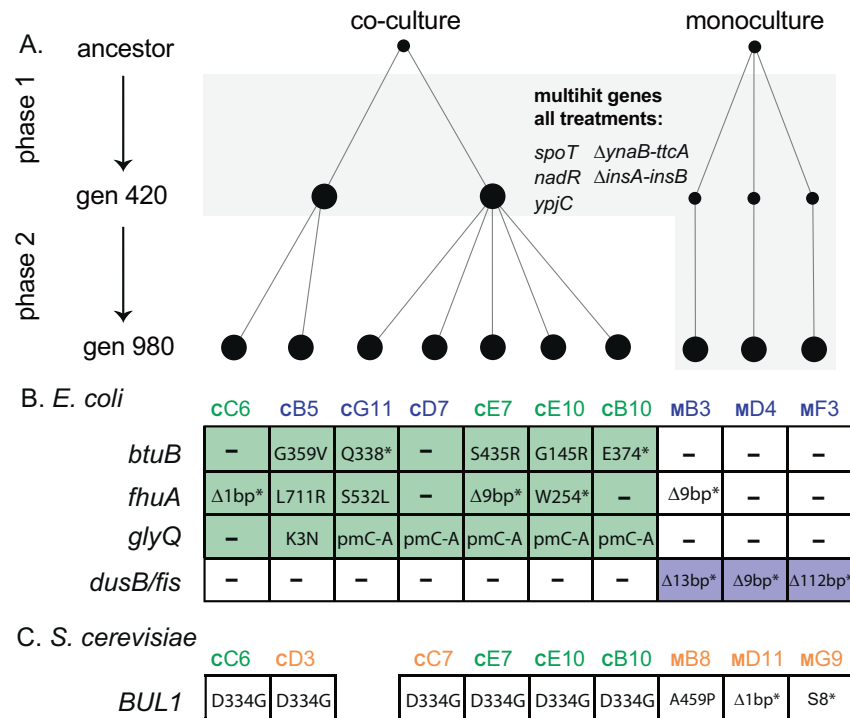


Fig. 3 The genetic causes of co-culture and monoculture specific evolution. **A** *E. coli* and *S. cerevisiae* populations from co-cultures were sequenced after 420 (two populations) and 980 generations (*E. coli* = seven and *S. cerevisiae* = six populations) and monoculture populations were sequenced after 980 generations (three populations) (Supplementary Data). In *E. coli*, mutations in five genes were found to be at high frequencies in all populations (A, grey shaded area). **B** Six independent mutations were found across the co-culture evolved populations in *btuB* and *fhuA* and two in *glyQ*. Population E10 had two mutations in both *btuB* and *fhuA*. All three monoculture populations

had unique mutations in the *dusB/fis* operon. **C** *BUL1* was mutated in all sequenced *S. cerevisiae* populations. Coloured text indicates the species present at generation 980. *E. coli* and *S. cerevisiae* (green text), *E. coli* only (blue text), *S. cerevisiae* only (orange text). Alphanumeric population codes (e.g., cC6) denote whether the population was evolved in coevolution (C) or monoculture (M) conditions and the position in the 96-well plate. “pm” indicates promoter, “*” indicates early stop or nonsense mutations. “-” indicates that no mutation was discovered in that gene.

The *btuB* and *fhuA* genes both contain a variety of non-synonymous mutations, including missense and nonsense mutations across the four co-cultured populations sequenced (Fig. 3), indicating selection for loss of function in these genes.

***BUL1* mutations in *S. cerevisiae* and *glyQ* mutations in *E. coli* are beneficial in monoculture growth conditions**

To measure the phenotypic effect of mutation of our single multi-hit *S. cerevisiae* gene, we engineered an allele that evolved in *BUL1* into the *S. cerevisiae* genetic background, and found an increase in growth rate that matched the increase in growth rate observed in the co-culture evolved yeast (post-hoc *t*-test, $p < 1 \times 10^{-4}$) (Fig. 4). To test the effect of the mutations discovered in *E. coli* multi-hit genes, we engineered deletions of *fhuA* and *btuB* into an ancestral strain of *E. coli* and reconstructed the evolved mutations of three clones from two of the coevolved populations that had occurred in the *btuB*, *fhuA*, and *glyQ*.

Where possible, we created single, double, and triple mutant combinations to measure combinatorial effect of mutations, although we had difficulty engineering *glyQ* (an essential gene) mutations into some genetic backgrounds. In order to check whether we had missed any mutations that could impact fitness, we also engineered the wild-type version of alleles for these three genes into evolved clones. In total, this was 22 separately engineered clones with different mutations in a range of combinations. We measured the growth of each of these mutants compared to the ancestral strains and found that *glyQ* mutations could account for a significant proportion of fitness increase in *E. coli* (post-hoc *t*-test, $p < 1 \times 10^{-4}$) (Fig. 5A). To check whether other genes aside from the three we checked were important for fitness, we replaced mutant alleles in the evolved strains with wild-type alleles. This revealed that while a mutant *glyQ* allele was necessary for high fitness it was not sufficient, suggesting the importance of other mutations or epistatic interactions that we have not identified (Fig. 5A). Interestingly, mutations in *fhuA* and *btuB* reduced growth compared to the

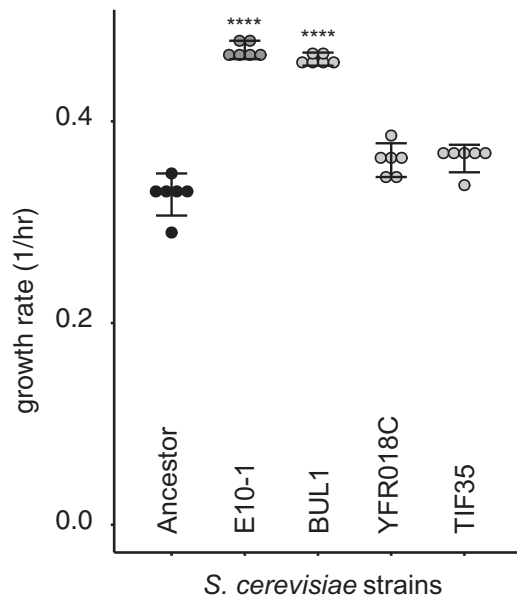


Fig. 4 Amino acid substitutions from BUL1 (D334G), YFR018C (L7F), and TIF35 (V272L) were engineered into the ancestral genetic background of *S. cerevisiae* (“Methods”). Growth rates were measured for the *S. cerevisiae* ancestor, the co-culture evolved *S. cerevisiae* clone E10-1 and the engineered three mutants. Stars indicate a significant difference from the ancestor (Bonferroni-corrected post-hoc *t*-tests).

ancestral strain (post-hoc *t*-test, $p < 1 \times 10^{-4}$) (Fig. 5A) but did not have a significant effect on competitive fitness (Supplementary Fig. 1).

Mutations in *E. coli* genes *fhuA* and *btuB* alter co-culture dynamics with *S. cerevisiae*

We tested whether engineered *E. coli* strains could invade ancestral and co-culture evolved *S. cerevisiae* (Fig. 5B, Supplementary Fig. 2). We found that mutations that disrupt *fhuA* and *btuB* were sufficient to change the equilibrium frequency of co-cultures. The capacity to reduce community stability was dependent on both the gene that had been ablated, and the *S. cerevisiae* genotype (Fig. 5B). For instance, co-culture-evolved *S. cerevisiae* B10 formed stable co-cultures with the *E. coli* ancestor from a range of starting frequencies, and similarly stable co-cultures with the *E. coli btuB* mutant (post-hoc *t*-test, $p > 0.05$). However, co-culture-evolved *S. cerevisiae* B10 was less able to coexist with the *fhuA* mutant (post-hoc *t*-test, $p = 4.5 \times 10^{-3}$). Notably, the evolved B10 co-culture *E. coli* did not have a mutation in *fhuA*. When the mutant *E. coli* is paired with evolved *S. cerevisiae* C6, stability is completely disrupted for *btuB* and *fhuA* so that different equilibria are reached (post-hoc *t*-test, $p < 1 \times 10^{-4}$). Even though the *E. coli* mutations do not increase competitive fitness against the *E. coli* ancestor, they were able to

disturb mechanisms of coexistence and increase the capacity for *E. coli* to competitively exclude co-culture evolved *S. cerevisiae*.

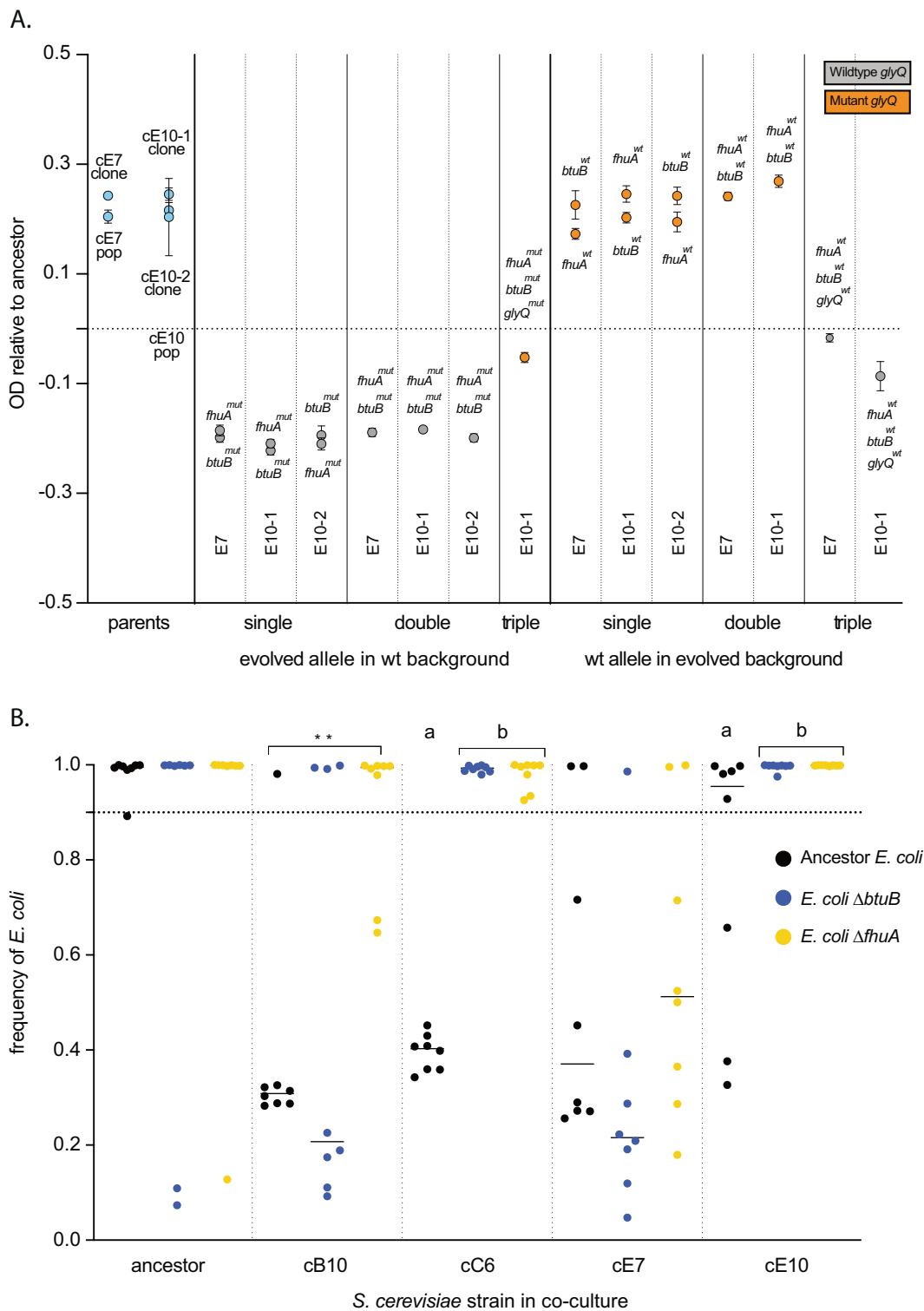
E. coli and *S. cerevisiae* evolved improved performance on spent media

We tested the idea that *S. cerevisiae* and *E. coli* had evolved to occupy different niches by carrying out growth experiments in spent medium. If *S. cerevisiae* can grow in medium that has been exhausted by a culture of *E. coli* (and the *E. coli* cells subsequently removed), this would suggest that *S. cerevisiae* can utilise a resource in the growth medium that cannot be accessed by *E. coli* or that *E. coli* produces a resource that can be utilised by *S. cerevisiae*. We found that ancestral *E. coli* and *S. cerevisiae* could not grow in medium previously exhausted by their own species, but both could grow on the spent medium of the other (Supplementary Figs. 3 and 4). After 980 generations of evolution, all of the co-culture evolved *E. coli* had an improved growth rate on the spent medium of its evolved partner *S. cerevisiae* strain (Fig. 6A), having a shorter lag phase than ancestor *E. coli* growing on *S. cerevisiae* spent medium and of which, three had evolved an increased carrying capacity (Supplementary Fig. 5). When we tested co-culture evolved *S. cerevisiae* on the spent medium of the *E. coli* they had coevolved with, only two of the co-culture-evolved *S. cerevisiae* had higher OD and none had a shorter lag phase (Supplementary Fig. 6).

We next tested whether *btuB* or *fhuA* mutations in *E. coli* conferred a growth advantage in spent medium from *S. cerevisiae* (Fig. 6). We found that the *fhuA* mutant had a significantly increased growth rate (post-hoc *t*-test, $p = 6 \times 10^{-4}$) (Fig. 6A); while *btuB* was not significantly different to the ancestor (post-hoc *t*-test, $p = 0.56$).

Evolved mutations in *fhuA* cause resistance to the antibiotic albomycin

While the selective benefit of *glyQ* is apparent in monoculture (Fig. 5A), the effects of *fhuA* and *btuB* mutations are specific to co-culture with *E. coli* and spent medium. The primary role of the FhuA and BtuB outer membrane transporters is to import ferrichrome and vitamin B12. However, both are also implicated in the transport of bacterial toxins (bactericins), are binding sites for bacteriophage, and FhuA imports the antibiotics albomycin and rifamycin. BtuB and FhuA depend on the periplasmic membrane protein TonB to provide energy for transport, and compete with five other *E. coli* outer membrane transporters for access to TonB. We hypothesised that the mutations in *btuB* and *fhuA* could prevent the binding of the cognate substrate. To test whether *fhuA* mutations are



altering the potential for taking up substrates, we measured the effect of an antibiotic, albomycin, that depends on binding *fhuA* for entry into the cell (Fig. 6B). We found that all of the evolved variants of *fhuA* were sufficient to confer

resistance to albomycin (post-hoc *t*-test, $p < 1 \times 10^{-4}$) (Fig. 6B). This suggests that the loss of *fhuA* substrate binding is important for improved growth of *E. coli* in co-culture with *S. cerevisiae*.

◀ **Fig. 5 The genetic causes of *E. coli* adaptation.** **A** Mutations in the essential gene *glyQ* cause the improved growth of evolved *E. coli* compared to ancestor *E. coli*. Growth was measured as OD₆₀₀ attained after 24 h of incubation at experimental conditions. Each dot represents a distinct engineered clone, where either one, two, or three alleles were altered. In one example, the two grey dots in the column indicated “evolved allele in wt background, single, E7” denote two separate strains where the ancestor *E. coli* genotype was engineered to carry either the *fhuA* or *btuB* mutant alleles that evolved in the E7 co-culture *E. coli*. For a second example, the single grey dot in the right-most column indicated “wt allele in evolved background, triple, E10-1” denotes engineering of an *E. coli* clone from the E10 co-culture evolved population. Here three mutant alleles (*fhuA*, *btuB*, and *glyQ*) were replaced with the wild-type alleles. The growth of each measured strain is plotted relative to the ancestor, which is set at 0, (the dotted line), all measured strains were judged significantly different from the ancestor using bonferroni-corrected post-hoc *t*-tests, $p < 0.001$. Error bars represent standard error of the mean (SEM). **B** The final equilibrium frequency of ancestral and mutant *E. coli* co-cultured with ancestor and co-culture evolved *S. cerevisiae* populations after a reciprocal invasion assay (**B**). The equilibrium frequency of the ancestor *E. coli* when co-cultured with each of these *S. cerevisiae* populations is shown (black dots). Also shown are mutant *E. coli* engineered to contain either a *btuB* (blue dots) or *fhuA* mutation (yellow dots). Each dot represents a single replicate co-culture experiment. Stars show significant differences between individual comparisons; lower case letters show significantly different groups as designated by the Tukey’s post-hoc test.

Discussion

Competitive exclusion sets a time limit for the evolution of coexistence

While previous evolution experiments have shown that how a single species can diversify into multiple coexisting ecotypes, the evolution of coexistence in this experiment is a relatively rare outcome (Fig. 1). In *E. coli*, 9 of 12 populations evolved coexisting ecotypes for tens of thousands of generations during a 61,500 generation experiment [44]. In *P. fluorescens*, the Wrinkly Spreader type evolves within a week whenever grown in non-shaken conditions [19]. Similarly, in a 1000 generations experiment with *S. cerevisiae*, 100 out of 1000 populations evolved an adherent type that coexisted with the progenitor ecotype [21, 45].

One factor working against the evolution of coexistence is the time limit set by the rate of competitive exclusion. Evolution experiments in a range of species have shown how ecological change can occur fast enough to change the selective conditions experienced by a population or community, and therefore drive further evolution [8, 10, 12, 15]. However, even rapid evolution of the more poorly adapted species does not always lead to stable coexistence [14]. In experiments founded from a single species, there is no time limit on evolutionary change in favour of coexistence, because a novel ecotype always has the potential to evolve via spontaneous mutation [44]. By contrast, in this experiment, *S. cerevisiae* must evolve the characteristics necessary to

promote coexistence before it is driven extinct by *E. coli*. In other words, interspecific competition is much stronger than intraspecific competition. This constraint might be expected to limit the potential for stable microbial communities to evolve from competing species. However, evolution in natural microbial communities might not operate under such constraints. For instance, competitive exclusion of one species will only cause local or temporary extinction of the weaker species. Future immigration events can provide further opportunities for the two species to co-habit, and co-evolve the mechanisms vital to coexistence. This suggests that the propensity for competing species to evolve coexistence may be increased by the presence of reservoir populations, potentially in stratified sub-sections of the environment, to provide multiple “trials” for the evolution of coexistence.

Genetic evolution in both *S. cerevisiae* and *E. coli* underpins coexistence

Our fitness measurements showed that the few *S. cerevisiae* that evolved to persist in co-culture with *E. coli* had a higher competitive fitness than monoculture evolved *S. cerevisiae*. *E. coli* on the other hand had similar increases in fitness in monoculture and co-culture (Fig. 2). While we did not find any co-culture specific genetic changes in *S. cerevisiae*, we did find one change consistent to all populations, suggesting that *S. cerevisiae* adaptations may have caused general increases in growth rate that were not dependent on the presence of *E. coli*. Crucially, co-culture evolved *S. cerevisiae* formed stable co-cultures with ancestral *E. coli*, while co-culture evolved *E. coli* rapidly outcompeted ancestral *S. cerevisiae* (Fig. 2C, D). This result suggests that the genetic changes in co-culture evolved *S. cerevisiae* were sufficient for coexistence.

Despite this result, we found strong evidence of co-culture specific adaptation in *E. coli* populations. All of the co-culture evolved *E. coli* had significantly improved growth in *S. cerevisiae* spent medium. Our genome sequencing experiments also showed that a distinct set of *E. coli* genes were targets for selection in co-culture (Fig. 3). The engineered substitutions of mutant and wild-type *glyQ* alleles into wild-type and evolved *E. coli* showed that mutations in *glyQ*, and probably another unknown locus (Fig. 5A), were responsible for increased *E. coli* growth in unspent medium. However, engineered disruptions of *fhuA* and *btuB* genes in *E. coli* did not improve growth, or increase fitness compared to the ancestor *E. coli* (Fig. 5A).

Why then were these mutations so strongly selected in all co-culture populations? We found that deleting *fhuA* and *btuB* altered the outcomes of invasion assays with ancestral and evolved *S. cerevisiae* (Fig. 5B). Moreover, the *fhuA* mutant had significantly improved growth in *S. cerevisiae*’s spent growth medium (Fig. 6A). Our experimental evidence supports that the selective pressure driving the fixation of

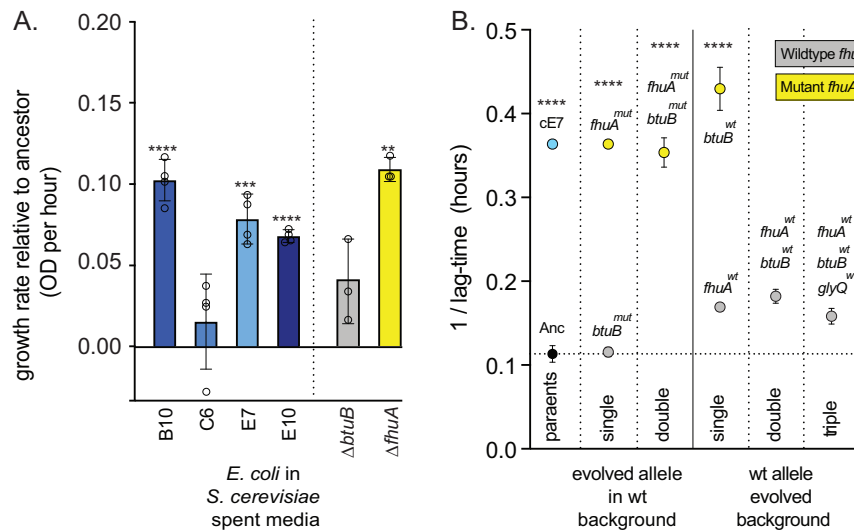


Fig. 6 Mutations in *fhuA* cause co-culture specific adaptation. **A** The co-culture evolved *E. coli*, and $\Delta fhuA$ mutant, have improved growth in spent medium relative to the *E. coli* ancestor. Each *E. coli* population was grown on spent medium from its respective co-culture *S. cerevisiae*. *E. coli* $\Delta btuB$ and $\Delta fhuA$ mutants were grown on spent medium from a culture from the co-culture evolved “E7” population of

S. cerevisiae. Error bars represent standard error of the mean (SEM). Stars show significant differences between strain growth in ancestor and evolved spent medium using post-hoc *t*-tests. **B** The change in lag-time for ancestral, coevolved, mutant and wild-type revertant strains when grown in the presence of the FhuA-targeting antibiotic albomycin. Error bars represent standard deviation (SD).

btuB and *fhuA* mutations emerged from interactions with *S. cerevisiae*.

***S. cerevisiae* persistence in co-culture led to rapid co-culture specific *E. coli* evolution**

The evolution of stable co-culture depends strongly on the genotype of both *E. coli* and *S. cerevisiae*. We expected rapid adaptation in *S. cerevisiae* in order to ameliorate or avoid direct interactions with *E. coli* that reduce fitness. However, it was surprising that *E. coli* evolved so many co-culture specific genetic changes, since *E. coli* was the fitter of the two species initially. We propose that in the rare cases where *S. cerevisiae* adapted quickly enough to coexist with *E. coli*, *S. cerevisiae* imposed strong selective pressures on *E. coli* to access new nutrients or avoid suppression, driving co-culture specific adaptations in *E. coli* and subsequently stabilising coexistence. This could explain why *S. cerevisiae* adaptations were general to both treatments of this experiment, but *E. coli* has multiple co-culture specific adaptations. Whole-genome sequencing in *S. cerevisiae* revealed that despite the discovery of many mutations across the genome, very few were in the same multi-hit genes (Supplementary Data). This may be because of the broad number of mutational targets available for *S. cerevisiae* to improve growth in high glucose medium. While our growth assays with engineered BUL1 mutants confirm the presence of a beneficial mutation in evolved yeast populations, future work will determine any other genetic causes of adaptation in the *S. cerevisiae* populations.

Molecular causes for the evolution of coexistence

Previous studies have found that microbial communities growing in rich medium are likely to produce toxic compounds that inhibit each other’s growth [46]. Since mutations in *fhuA* and *btuB* are known to provide resistance to bacteriocins [47], it is possible that the mutations discovered in this study provide resistance to a secreted product of *S. cerevisiae*. However, while some *S. cerevisiae* strains secrete antimicrobial peptides [48], our data do not suggest any candidates for such a secreted molecule. A second explanation is related to the role of the FhuA and BtuB proteins as two of seven membrane transporters that depend on TonB to provide the energy for substrate transport [49]. TonB dependent transporters compete for access to TonB [50], and we found that the mutations that evolved in our study render FhuA insensitive to its cognate substrate, and therefore unable to activate TonB. The inactivation of FhuA and BtuB would increase availability of TonB for other TonB-dependent transporters. If one or more of these transporters is in high use due to co-culture with *S. cerevisiae*, this would provide a selective advantage. In future work, we plan to carry out experiments to resolve these two hypotheses.

Conclusions

Here we have shown that a prokaryote and a eukaryote, that are mismatched in co-culture and are not known to cohabit in nature, can evolve to coexist. The adaptive

changes discovered in *E. coli* reinforce that evolution in the context of a community can be dramatically different to evolution in isolation. Most studies of microbial evolution, molecular biology, and antibiotic resistance have been carried out in monocultures; microbiology in co-culture could yield new insights into each of these areas of research.

Methods

Strains

The *E. coli* strain used to found the evolution experiment is isogenic with the laboratory strain *E. coli* MG1655 K-12 F⁻ λ *ilvG* *rfb-50* *rph-1*. The *S. cerevisiae* ancestor was haploid, non-recombining *S. cerevisiae* strain R1158 with genotype *trp1::Hph URA::CMV-tTA MATa his3-1 leu2-0met15-0* [51].

Medium composition

All strains were grown within a defined medium supplemented with 4% glucose, also called high-glucose medium (HGM), described in previous work [52].

Long-term evolution

To set up the evolution experiment, single clones of MG1655 and R1158 were grown to saturation in high-glucose medium, diluted 1:2¹⁰ and used to seed 60 replicate co-culture populations in a single 96-well plate, as well as 30 replicate populations for each species in monoculture in a separate 96-well plate. The cultures were evolved through 420 generations (42 daily cycles) of growth and dilution in high-glucose medium at 28 °C and 750 RPM. Every 24 h, the populations were diluted 1:2¹⁰ by serially diluting 1:2⁵ (4 μ L into 125 μ L) \times 1:2⁵ (4 μ L into 125 μ L) into new high-glucose medium. All dilutions were performed using the Hamilton96 Liquid Handler with the CO-RE 96 Probe Head. After every 70 generations, populations were mixed with 50 μ L of 75% glycerol and archived at -80 °C. At 420 generations, single clones of each co-culture species were extracted from wells C3 and B4 of the co-culture 96-well plate by plating onto selective agar, grown to saturation in high-glucose medium at 28 °C, and used to found 60 replicate co-culture populations in a new 96-well plate. All monoculture population lineages continued to be propagated after 420 generations. Both monoculture and co-culture populations were evolved for a further 580 generations (58 daily cycles) under the same conditions, for a total of ~1000 generations of growth (100 daily cycles).

Stable frequency assay

Single colonies of each ancestor were grown on YPD agar, and one colony was picked from each ancestral population. These individual colonies were grown to saturation in 3 mL of defined supplemented medium. Ancestral *E. coli* and ancestral *S. cerevisiae* were mixed together and propagated together under long-term evolution conditions as outlined above for 70 generations, along with population samples of each co-culture at 1000 generations. In conjunction with the continual growth and dilution of evolving cultures, populations were also diluted 1:10 and 1:100 (13 μ L in 119 μ L \times 13 μ L in 119 μ L) into 1 \times phosphate-buffered saline for measurement of total cell count using flow cytometry. Nine microliters samples were taken from each population for cell counts, with a maximum total count of 30,000 events.

Competitive fitness assays

For fitness assays of evolved *E. coli* populations, we selected 35 co-culture populations and 30 monoculture populations to measure their fitness relative to a GFP-expressing reference *E. coli* strain. For fitness assays of evolved *S. cerevisiae* populations, we selected all remaining co-culture populations (seven total) and 30 monoculture populations to measure their fitness relative to a GFP-expressing reference *S. cerevisiae* strain.

Experimental and reference strains were grown to saturation in separate 15 mL falcon tubes. If the strains to be tested were coming from the -80 °C freezer, strains were passaged further by diluting 1:2⁵ in a 96-well plate to re-acclimatise to the appropriate medium. Experimental and reference strains were mixed 25 μ L:75 μ L (1:3) manually, before propagating for 20 generations (two daily cycles) using the Hamilton96 Liquid Handler. In conjunction with the continual growth and dilution of evolving cultures, populations were also diluted each day 1:10 and 1:100 (13 μ L in 119 μ L \times 13 μ L in 119 μ L) into 1 \times phosphate buffered saline for measurement of total cell count by flow cytometry using a LSR Fortessa X20a. Nine microliters samples were taken from each population for cell counts, with a minimum count of 10,000 events, and a maximum total count of 30,000 events.

For fitness assays of mutant *E. coli* populations, the same competitive fitness assay protocol was used, but with the following changes. Instead of population samples, clonal samples of ancestral, mutant, and coevolved populations were taken from single colonies grown on YPD agar.

Whole-genome sequencing

For sequencing clones, we used single colonies grown on YPD agar and picked one colony from each population to

sequence at two time points. These individual colonies were grown to saturation in 3 mL of defined supplemented medium and total genomic DNA was isolated for each sample the GenElute bacterial DNA prep kit (Sigma-Aldrich). DNA concentrations were measured on a Qubit analyser and sent to Genewiz (NJ, USA) for library preparation and short-read sequencing on a HiSeq X-10 (illumina). Upon receipt of fastQ files, variants were called using Breseq v.0.33.2, using default parameters [53]. Each *E. coli* sample was aligned to the complete and annotated MG1655 genome sourced from NCBI, and each *S. cerevisiae* sample was aligned to the complete and annotated R1158 genome sourced from NCBI. Each sample was sequenced to a depth of $\sim 100\times$ coverage for *E. coli* and $\sim 50\times$ coverage for *S. cerevisiae*. Outputs were aligned together using the gdttools. COMPARE function within breseq used to determine which mutations were unique or shared across monoculture and co-culture populations. Single nucleotide polymorphisms at or above 40% frequency were used for analysis of genomic alterations.

***S. cerevisiae* growth assay**

Single colonies were grown on YPD agar, and one colony was picked from ancestral, evolved E10 and mutant populations. These individual colonies were grown in 10 mL non-shaking HGM for 24 h [54]. All strains were standardised to 0.01 OD₆₀₀ using HGM as diluent and placed into 96-well microplates ($n = 6$). Growth of each population monitored by tracking optical density (OD) of cultures in a plate reader for 24 h, with readings taken every 10 min. The resultant growth data were fitted to logistic curves using the R package growthcurver to calculate growth rates, r , of each strain [55].

Invasion assay

Single colonies were grown on YPD agar, and one colony was picked from each ancestral, evolved and mutant population. These individual colonies were grown to saturation in 3 mL of defined supplemented medium. *E. coli* and *S. cerevisiae* were mixed together at different volumetric ratios and correlated with total cell count using flow cytometry. From this a range of ratios was created by mixing *E. coli* and *S. cerevisiae* together in different volumetric ratios across 3, 96-well plates, ranging from 9:1 to 1:9 (*E. coli*:*S. cerevisiae*). This initial mix plate then underwent long-term evolution transfer conditions as outlined above, except instead of evolving populations for 1000 generations (100 daily cycles), populations were evolved for 140 generations (14 daily cycles). In conjunction with the continual growth and dilution of evolving cultures, populations were also diluted 1:10 and 1:100

(13 μL in 119 μL \times 13 μL in 119 μL) into 1 \times phosphate-buffered saline for measurement of total cell count using flow cytometry. Nine microliters samples were taken from each population for cell counts, with a maximum total count of 30,000 events.

Spent medium assay

To generate spent medium for ancestral samples, single clones of ancestral MG1655 and ancestral R1158 were grown to saturation in 3 mL of high-glucose medium at 28 °C over 24 h. Cells were removed from overnight cultures via centrifugation (10,000 rpm for 2 min) and supernatant removed. Cells were washed in phosphate-buffered saline via centrifugation before being resuspended in 3 mL phosphate-buffered saline. Supernatant was filter sterilised through a syringe filter with a pore size of 0.2 μm . Filtered spent medium was then added to a 96-well plate, with 128 μL per well. Four microliters of resuspended cells was then added to spent medium. Each species was added to both its own species spent medium and the opposite species spent medium in four replicates each. Growth of each population monitored by tracking OD of cultures in plate reader for 24 h, with readings taken every 20 min. Growth conditions were the same as long-term evolution experiment. Maximum OD, time to exponential phase (defined as OD greater than 0.1), and maximum growth rate (calculated over five data points) recorded.

For spent medium assays with evolved population samples, mixed population samples of each evolved population were grown in 3 mL of defined medium overnight, with antibiotics to remove either *S. cerevisiae* (cycloheximide) or *E. coli* (tetracycline). Ten microliters of culture then plated onto non-selective agar and incubated. Multiple colonies from agar plate picked from plate and regrown in 3 mL of defined medium without antibiotics. The same sterilisation and filtration procedure was followed to generate spent medium and resuspended cells. Each evolved strain was grown in ancestral and evolved spent medium of both MG1655 and R1158.

For spent medium assays of *E. coli* mutant strains, single colonies of each mutant selected was grown overnight in 3 mL of high-glucose medium at 28 °C over 24 h, before being centrifuged, washed and resuspended as outlined above. The same sterilisation and filtration procedure was followed to generate spent medium and resuspended cells. Each *E. coli* mutant strain was grown in ancestral and evolved spent medium of R1158.

Albomycin growth assays

Both population and clonal samples of evolved strains were grown overnight in 3 mL of high-glucose medium at 28 °C

over 24 h, as well as single clones of each mutant and wild-type revertant strains. Overnight cultures were diluted 1:2¹⁰ by serially diluting 1:2⁵ (4 µL into 125 µL) × 1:2⁵ (4 µL into 125 µL) into new high-glucose medium in a 96-well plate. Growth of each population monitored by tracking OD of cultures in plate reader for 24 h, with readings taken every 20 min. Maximum OD, time to exponential phase (defined as OD greater than 0.1), and maximum growth rate (calculated over 5 data points) recorded.

For growth curves with additional albomycin, the same protocol was used as outlined above, with the following changes. Overnight cultures were diluted 20-fold in 1 mL of PBS (50 µL into 950 µL) before a further 50-fold dilution into 200 µL of high-glucose medium with 50 mg/mL albomycin.

Statistical methods

All statistical tests conducted were one way ANOVA with Bonferroni-corrected post-hoc *t*-tests (*p* values <0.05*, 0.01**, 0.001***, and 0.0001****) or tukey's post-hoc tests (groups shown by letters), except where otherwise specified.

E. coli strain modifications

Strain constructions were carried out using CRISPR-Cas for *E. coli*, adopted from Jiang et al. [56]. Both pTargetF (guide RNA expressing, Plasmid #62226) and pCas (Cas9 expressing, Plasmid #62225) plasmids were obtained from Addgene. *E. coli* Top10 cells were used as a cloning host and genetic changes were introduced into the ancestral MG1655 strain. Further, we have swapped mutant alleles with the wild-type alleles (from the ancestor) in the selected evolved clones.

Modification of 20 N sequence in pTargetF

Target sequences were chosen for each gene using the online tool CCTop [57] (Supplementary Table 1). Plasmid modifications were carried out in three steps. Step 1 was the removal of 20N sequence from pTargetF. Plasmid pTargetF was cut with SpeI and PshAI restriction enzymes, then the fragment containing the backbone of the plasmid without 20N sequence was gel purified. Step 2 was the construction of DNA fragments with new 20 N sequence. PCR fragments with 20N target sequences for each gene were generated in three PCR reactions. First, PCR fragment was amplified using pTargetF-F1 and pTargetF-R1 primers (R1 primers have reverse complement of 20N sequence specific to each gene at the 5'-end) (see Supplementary Table 2 for primers). Second, PCR reactions used pTargetF-F2, with 20N sequence for each gene at the 5'-end, and pTargetF-R2

primers. These two PCR fragments were gel purified and used as templates in the third PCR with the outer primers (pTargetF-F1 and pTargetF-R2) to generate a PCR fragment with a 20N sequence. Later, the third PCR fragments were also cut with SpeI and PshAI restriction enzymes to generate complementary ends to the plasmid backbone. Step 3 involved insertion of plasmid with 20N target sequence into cloning host cells. Plasmid backbone from step 1 and DNA fragments with the new 20N sequences from step 2 were ligated using instant Sticky-end Ligase Master Mix (NEB) and electroporated with 50 µL electro-competent Top10 cells using 1-mm Gene Pulser cuvette (Bio-Rad), at 2.5 kV. Cells were recovered at 37° for 1 h before being spread onto LB agar plates containing spectinomycin (50 mg/L). Sanger sequencing confirmed the presence of colonies with the modified pTargetF plasmids, namely; trpF pTargetF, tonB pTargetF, fhuA pTargetF, btuB1 pTargetF, btuB2 pTargetF, and ampR pTargetF.

Repair DNA constructions

CRISPR engineering requires a donor "repair" DNA that the cell will use to repair the cut target side, thereby introducing the desired DNA sequenced change.

eGFP strain

A 50 base pair cloning strategy was used for the construction of GFP-containing fragment. The *trpF* gene was targeted (with *trpF* pTargetF) as a GFP insertion site. GFPmut2 DNA was amplified from pMGS053 plasmid using GFP-F and GFP-R primers (see Supplementary Table 2). The resultant DNA fragment had 50 base pair homologies at both 5' and the 3'-ends corresponding to the upstream and downstream of 20 N sequence in *trpF* gene.

fhuA mutants

The *fhuA* mutant allele swap was generated by swapping this gene with AmpR cassette, then swapping *ampR* cassette with the exact mutations seen in the evolution experiment. In the first stage, *fhuA* pTargetF plasmid was used to direct Cas9 enzyme to introduce double strand breaks in *fhuA* gene. Then, *fhuA ampR* cassette DNA fragment was used as repair DNA. This DNA fragment was constructed with 400 to 600 base pair homologies of upstream and downstream of *fhuA* gene. *ampR* gene (including its promoter and terminator sequences) was amplified from pUC19 plasmid using ampR-F and ampR-R primers. 5'-end of these primers were designed to generate homology (about 20 bp) to upstream and downstream of *fhuA*. Upstream sequence was amplified with fhuA-F1 and fhuA-R1 and downstream sequence was amplified with fhuA-F2 and fhuA-R2 primers

(Supplementary Table 2) using MG1655 DNA as a template. Finally, overlap PCR method was used to join the three DNA fragments. This stage results in a knock-out mutant. In the second stage, *ampR* cassette was targeted by Cas9 enzyme (with *ampR* pTargetF) and swapped with repair DNA containing exact mutations for *fhuA*. A colony PCR was used to amplify repair DNA using evolved clones as template DNA and *fhuA*-F1, *fhuA*-R2 primer pairs (see Supplementary Table 2).

***btuB* mutants**

A deletion strategy in two stages was used for the *btuB* mutant construction. In the first stage, Cas9 enzyme was directed to a site in the *btuB* gene with *btuB1* pTargetF plasmid. Then, a deletion repair DNA fragment was used to introduce the deletion. This DNA fragment was generated with three PCR reactions. The first PCR step used *btuB*-F1 and *btuB*-R1 primers (Supplementary Table 2) and MG1655 template DNA resulting in a DNA fragment containing upstream and downstream of start codon of *btuB*. The second step used *btuB*-F2 (containing the forward sequence of *btuB*-R1 at 5'-end to generate homology between the two PCR fragments) and *btuB*-R2 primers (Supplementary Table 2) to amplify upstream of *btuB* stop codon (making sure *murI* start codon is undisturbed) and downstream sequence. The third step used these two PCR fragments as template DNA and *btuB*-F1 and *btuB*-R2 primers to generate a repair DNA fragment resulting in a 1386 bp deletion in the middle section of *btuB* gene. In the second stage, a 20 N sequence targeted the location where the two PCR fragments fused (see above) with the *btuB2* pTargetF. Then a DNA fragment was amplified using *btuB*-F1, *btuB*-R2 primer pair with an evolved clone as template and used as a repair DNA to introduce *btuB* mutations from the evolution experiment to ancestral MG1655 cells.

***glyQ* mutants**

glyQ is an essential gene and its modification requires a different two stage CRISPR strategy as its inactivation results in cell death. In the first stage, *ampR* cassette was carefully inserted upstream of *glyQ* promoter, leaving the promoter undisturbed. No pTargetF plasmid was used to introduce double strand breaks at this location [58]. A *glyQ ampR* cassette DNA fragment was generated with a four step PCR protocol. In the first step, upstream of the promoter was amplified using *glyQ*-F1 and *glyQ*-R1 primers (Supplementary Table 2). In the second step *glyQ*-F2 and *glyQ*-R2 primers were used to amplify the region that includes few bases upstream of the promoter, *glyQ* start codon and partial *glyQ* sequence following downstream of the start codon. *ampR* cassette was then amplified from

pUC19 plasmid using *glyQ*-amp-F and *glyQ*-amp-R primers in the third step (Supplementary Table 2). Finally, the resulting three PCR fragments were merged in a fusion PCR using *glyQ*-F1 and *glyQ*-R2 primers. In the second stage of CRISPR, *ampR* cassette was targeted with *ampR* pTargetF and the cassette was deleted with the insertion of the new repair DNA (amplified with *glyQ*-F1, *glyQ*-R2 primer pair and evolved clone template DNA) containing the evolved *glyQ* promoter mutation.

Wild-type allele revertants

The same two stage CRISPR strategy was used to swap evolved alleles with the ancestral alleles in the evolved *E. coli* clones: E10-1, E10-2, and E7 for *fhuA*, *btuB*, and *glyQ* genes. In the first stage, evolved alleles were swapped with the *ampR* cassette, before being swapped with the wild-type ancestral allele in the second stage. For *glyQ* this *ampR* cassette was inserted in front of the *glyQ* promoter region.

CRISPR-Cas system transformations

Ancestral MG1655 cells were first transformed with pCas plasmid via electroporation. Cells harbouring pCas grown overnight before a 1 in 100 v/v dilution in medium including kanamycin (50 mg/L). After allowing them to grow for 2 h, λ -Red recombination genes were induced with arabinose (10 mM final concentration) addition. Cells were allowed to grow for another hour and made electro-competent as described previously [59]. Fifty microliters of cells mixed with 100 ng of modified pTargetF plasmids and 1–5 μ g of repair DNAs in a 1-mm Gene Pulser cuvettes (Bio-Rad) at 2.5 kV. Cells resuspended in 1 mL of LB medium and allowed to recover at 28 °C for 1 h before being spread onto LB agar plates containing kanamycin (50 mg/L) and spectinomycin (50 mg/L) and incubated at 28 °C overnight. The presence of mutations confirmed with colony PCR and Sanger sequencing.

***S. cerevisiae* strain modifications**

Strain constructions were carried out using CRISPR-Cas for *S. cerevisiae*, following methods from DiCarlo et al. [60] and Biot-Pelletier and Martin [61]. Both p426-SNR52p-gRNA.CAN1.Y-SUP4t (guide RNA expressing, Plasmid #43803) and p414-TEF1p-Cas9-CYC1t (Cas9 expressing, Plasmid #43802) plasmids were obtained from Addgene. *E. coli* Top10 cells were used as a cloning host and genetic changes were introduced into the ancestral strain R1158.

As R1158 grows in synthetic media lacking uracil, URA3 marker was changed to a LEU2 marker in p426 plasmid as follows. First, the LEU2 marker was amplified

from p415-Gall-Cas9-CYC1t (Addgene, Plasmid #43804) using p415-Leu-F and p415-Leu-R primers (Supplementary Table 2). Second, the backbone of p426 plasmid was amplified using p426-minus-Ura-F and p426-minus-Ura-R primers. Third, we have assembled first two PCR fragments using Circular Polymerase Extension Cloning (CPEC) [62]. Finally, 5 μ L of CPEC product was electroporated with 50 μ L electro-competent Top10 cells using 1-mm Gene Pulser cuvette (Bio-Rad), at 2.5 kV. Cells were recovered at 37 °C for 1 h before spreading onto LB agar plates containing ampicillin (50 mg/L). The resultant plasmid was called p426-LEU2.

Modification of 20 N sequence in p426-LEU2

Target sequences were chosen for each gene using the online tool CCTop [57] (Supplementary Table 1). Plasmid modifications were carried out in three steps. Step 1 involved the amplification of the backbone of the plasmid without 20 N sequence using p426-F1-reversed and p426-R2-reversed primers (Supplementary Table 2). Step 2 was the construction of DNA fragments with new 20 N sequence. PCR fragments with 20 N target sequences for each gene were generated in three PCR reactions. First PCR used p426-F1 and p426-R1 primers (R1 primers have reverse complement of 20 N sequence specific to each gene at the 5'-end (see Supplementary Table 2 for primers). Second PCR reactions used p426-F2, with 20 N sequence for each gene at the 5'-end, and p426-R2 primers. These two PCR fragments were gel purified and used as templates in the third PCR with the outer primers (p426-F1 and p426-R2) to generate a PCR fragment with a 20 N sequence. In the 3rd step, PCR fragments from step 1 and step 2 were assembled using CPEC [62] and electroporated into Top10 cells and confirmed with Sanger sequencing.

Repair DNA constructions

BUL1 and YFR018C mutants

Mutant alleles for BUL1 and YFR018C were generated in two successive CRISPR events. In the first event, a repair DNA containing 20 N stuffer sequence was inserted [61]. The stuffer repair DNA was generated in three PCR steps. The first PCR used gene-F1 and gene-R1 primers to amplify upstream of the stuffer insertion location. The second PCR used gene-F2 and gene-R2 primers to amplify downstream of the insertion location. Stuffer sequence was used to generate the required homology between the first and the second DNA fragments and the two fragments were joined in the 3rd PCR using gene-F1 and gene-R2 primers. Finally, the stuffer sequence was targeted using stuffer-p426-LEU2 plasmid and swapped

with the new repair DNA having exact mutations seen in the evolution experiment. Repair DNA was amplified with a colony PCR from the evolved clones using primers gene-F1 and gene-R2.

TIF35 mutant

TIF35 is an essential gene, requiring a one step CRISPR event. We chose a 20N target sequence such that NGG PAM sequence is the mutation site in the evolved clone. We have targeted this 20N sequence in the ancestor using TIF35-p426-LEU2 plasmid and provided the repair DNA from the evolved clones, amplified with using TIF35-F1 and TIF35-R1 primers.

All transformation events (plasmids and repair DNAs) were carried out using a standard lithium acetate transformation method [63]. The presence of mutations confirmed with colony PCR and Sanger sequencing.

Data availability statement

Raw sequencing reads have been deposited in the NCBI Biosample database with Bioproject ID: PRJNA668197

Acknowledgements MJM was supported by ARC Discovery Grant (DP180102161) and an ARC Future Fellowship (FT170100441).

Author contributions MJM conceived the study, JNB, ALS, JMV, TDA and MJM designed and carried out experiments, JNB, ALS, LCW and MJM analysed the data. JNB and MJM wrote the paper. All authors have read and approved the final manuscript.

Compliance with ethical standards

Conflict of interest The authors declare that they have no conflict of interest.

Publisher's note Springer Nature remains neutral with regard to jurisdictional claims in published maps and institutional affiliations.

References

1. Foster KR, Bell T. Competition, not cooperation, dominates interactions among culturable microbial species. *Curr Biol*. 2012;22:1845–50.
2. Gause GF. Experimental analysis of Vito Volterra's mathematical theory of the struggle for existence. *Science*. 1934;79:16–7.
3. Chesson P. Mechanisms of maintenance of species diversity. *Annu Rev Ecol Syst*. 2000;31:343–66.
4. Lankau RA. Rapid evolutionary change and the coexistence of species. *Annu Rev Ecol Evol Syst*. 2011;42:335–54.
5. Kawecki TJ, Ebert D. Conceptual issues in local adaptation. *Ecol Lett*. 2004;7:1225–41.
6. Hubbell SP. Neutral theory and the evolution of ecological equivalence. *Ecology*. 2006;87:1387–98.
7. MacArthur R, Levins R. The limiting similarity, convergence, and divergence of coexisting species. *Am Nat*. 1967;101:377–85.

8. Bailey JK, Hendry AP, Kinnison MT, Post DM, Palkovacs EP, Pelletier F, et al. From genes to ecosystems: an emerging synthesis of eco-evolutionary dynamics. *N Phytol.* 2009;184:746–9.
9. Baquero F, Blázquez J. Evolution of antibiotic resistance. *Trends Ecol Evol.* 1997;12:482–7.
10. Grant PR, Grant BR. Evolution of character displacement in Darwin's finches. *Science.* 2006;313:224–6.
11. Koepfel AF, Wertheim JO, Barone L, Gentile N, Krizanc D, Cohan FM. Speedy speciation in a bacterial microcosm: new species can arise as frequently as adaptations within a species. *ISME J.* 2013;7:1080–91.
12. Stuart YE, Campbell T, Hohenlohe P, Reynolds RG, Revell L, Losos J. Rapid evolution of a native species following invasion by a congener. *Science.* 2014;346:463–6.
13. Schulte RD, Makus C, Hasert B, Michiels NK, Schulenburg H. Multiple reciprocal adaptations and rapid genetic change upon experimental coevolution of an animal host and its microbial parasite. *Proc Natl Acad Sci USA.* 2010;107:7359–64.
14. Pimentel D, Feinberg EH, Wood PW, Hayes JT. Selection, spatial distribution, and the coexistence of competing fly species. *Am Nat.* 1965;99:97–109.
15. Hart SP, Turcotte MM, Levine JM. Effects of rapid evolution on species coexistence. *Proc Natl Acad Sci USA.* 2019;116:2112–7.
16. Traverse CC, Mayo-Smith LM, Poltak SR, Cooper VS. Tangled bank of experimentally evolved *Burkholderia* biofilms reflects selection during chronic infections. *Proc Natl Acad Sci USA.* 2012;110:250–9.
17. Turner CB, Marshall CW, Cooper VS. Parallel genetic adaptation across environments differing in mode of growth or resource availability. *Evolution Lett.* 2018;2:355–67.
18. Elena SF, Lenski RE. Microbial genetics: evolution experiments with microorganisms: the dynamics and genetic bases of adaptation. *Nat Rev Genet.* 2003;4:457.
19. Rainey PB, Travisano M. Adaptive radiation in a heterogeneous environment. *Nature.* 1998;394:69.
20. Ferguson GC, Bertels F, Rainey PB. Adaptive divergence in experimental populations of *Pseudomonas fluorescens*. V. Insight into the niche specialist fuzzy spreader compels revision of the model *Pseudomonas* radiation. *Genetics.* 2013;195:1319–35.
21. Frenkel EM, McDonald MJ, Van Dyken JD, Kosheleva K, Lang GI, Desai MM. Crowded growth leads to the spontaneous evolution of semistable coexistence in laboratory yeast populations. *Proc Natl Acad Sci USA.* 2015;112:11306–11.
22. Zuppinge-Dingley D, Schmid B, Petermann JS, Yadav V, De Deyn GB, Flynn DF. Selection for niche differentiation in plant communities increases biodiversity effects. *Nature.* 2014;515:108.
23. Le Gac M, Plucain J, Hindré T, Lenski RE, Schneider D. Ecological and evolutionary dynamics of coexisting lineages during a long-term experiment with *Escherichia coli*. *Proc Natl Acad Sci USA.* 2012;109:9487–92.
24. Rosenzweig RF, Sharp R, Treves DS, Adams J. Microbial evolution in a simple unstructured environment: genetic differentiation in *Escherichia coli*. *Genetics.* 1994;137:903–17.
25. Helling RB, Vargas CN, Adams J. Evolution of *Escherichia coli* during growth in a constant environment. *Genetics.* 1987;116:349–58.
26. D'Souza G, Kost C. Experimental evolution of metabolic dependency in bacteria. *PLoS Genet.* 2016;12:e1006364.
27. Oliveira NM, Niehus R, Foster KR. Evolutionary limits to cooperation in microbial communities. *Proc Natl Acad Sci USA.* 2014;111:17941–6.
28. Kallus Y, Miller JH, Libby E. Paradoxes in leaky microbial trade. *Nat Commun.* 2017;8:1361.
29. Muller EE, Faust K, Widder S, Herold M, Arbas SM, Wilmes P. Using metabolic networks to resolve ecological properties of microbiomes. *Curr Opin Syst Biol.* 2018;8:73–80.
30. Friedman J, Higgins LM, Gore J. Community structure follows simple assembly rules in microbial microcosms. *Nat Ecol Evol.* 2017;1:0109.
31. Harcombe WR, Betts A, Shapiro JW, Marx CJ. Adding biotic complexity alters the metabolic benefits of mutualism. *Evolution.* 2016;70:1871–81.
32. Harcombe WR, Chacón JM, Adamowicz EM, Chubiz LM, Marx CJ. Evolution of bidirectional costly mutualism from byproduct consumption. *Proc Natl Acad Sci USA.* 2018;115:12000–4.
33. Farrell JM, Brown SP. Evolution of bacterial trade in a two-species community. *Proc Natl Acad Sci USA.* 2018;115:11874–5.
34. Morris JJ. Black Queen evolution: the role of leakiness in structuring microbial communities. *Trends Genet.* 2015;31:475–82.
35. Lawrence D, Fiegna F, Behrends V, Bundy JG, Phillimore AB, Bell T, et al. Species interactions alter evolutionary responses to a novel environment. *PLoS Biol.* 2012;10:e1001330.
36. Goldford JE, Lu N, Bajić D, Estrela S, Tikhonov M, Sanchez-Gorostiaga A, et al. Emergent simplicity in microbial community assembly. *Science.* 2018;361:469–74.
37. Cordero OX, Ventouras L-A, DeLong EF, Polz MF. Public good dynamics drive evolution of iron acquisition strategies in natural bacterioplankton populations. *Proc Natl Acad Sci USA.* 2012;109:20059–64.
38. Adler PB, HilleRisLambers J, Levine JM. A niche for neutrality. *Ecol Lett.* 2007;10:95–104.
39. Paterson S, Vogwill T, Buckling A, Benmayer R, Spiers AJ, Thomson NR, et al. Antagonistic coevolution accelerates molecular evolution. *Nature.* 2010;464:275.
40. Buckling A, Rainey PB. Antagonistic coevolution between a bacterium and a bacteriophage. *Proc R Soc Lond Ser B: Biol Sci.* 2002;269:931–6.
41. Piccardi P, Vessman B, Mitri S. Toxicity drives facilitation between 4 bacterial species. *Proc Natl Acad Sci USA.* 2019;116:15979–84.
42. Goddard MR, Greig D. *Saccharomyces cerevisiae*: a nomadic yeast with no niche? *FEMS Yeast Res.* 2015;15:fov009.
43. Van Elsas JD, Semenov AV, Costa R, Trevors JT. Survival of *Escherichia coli* in the environment: fundamental and public health aspects. *ISME J.* 2011;5:173–83.
44. Good BH, McDonald MJ, Barrick JE, Lenski RE, Desai MM. The dynamics of molecular evolution over 60,000 generations. *Nature.* 2017;551:45.
45. Lang GI, Botstein D, Desai MM. Genetic variation and the fate of beneficial mutations in asexual populations. *Genetics.* 2011;188:647–61.
46. Ratzke C, Barrere J, Gore J. Strength of species interactions determines biodiversity and stability in microbial communities. *Nat Ecol Evol.* 2020;4:376–83.
47. Braun V. Energy-coupled transport and signal transduction through the gram-negative outer membrane via TonB-ExbB-ExbD-dependent receptor proteins. *FEMS Microbiol Rev.* 1995;16:295–307.
48. Branco P, Francisco D, Chambon C, Hebraud M, Arneborg N, Almeida MG, et al. Identification of novel GAPDH-derived antimicrobial peptides secreted by *Saccharomyces cerevisiae* and involved in wine microbial interactions. *Appl Microbiol Biotechnol.* 2014;98:843–53.
49. Noinaj N, Guillier M, Barnard TJ, Buchanan SK. TonB-dependent transporters: regulation, structure, and function. *Annu Rev Microbiol.* 2010;64:43–60.
50. Howard SP, Herrmann C, Stratilo CW, Braun V. In vivo synthesis of the periplasmic domain of TonB inhibits transport through the FecA and FhuA iron siderophore transporters of *Escherichia coli*. *J Bacteriol.* 2001;183:5885–95.
51. Hughes TR, Marton MJ, Jones AR, Roberts CJ, Stoughton R, Armour CD, et al. Functional discovery via a compendium of expression profiles. *Cell.* 2000;102:109–26.

52. Zhou K, Qiao K, Edgar S, Stephanopoulos G. Distributing a metabolic pathway among a microbial consortium enhances production of natural products. *Nat Biotechnol.* 2015;33:377.
53. Barrick JE, Colburn G, Deatherage DE, Traverse CC, Strand MD, Borges JJ, et al. Identifying structural variation in haploid microbial genomes from short-read resequencing data using bre-seq. *BMC Genom.* 2014;15:1039.
54. Hall BG, Acar H, Nandipati A, Barlow M. Growth rates made easy. *Mol Biol Evol.* 2014;31:232–8.
55. Sprouffske K, Wagner A. Growthcurver: an R package for obtaining interpretable metrics from microbial growth curves. *BMC Bioinform.* 2016;17:172.
56. Jiang Y, Chen B, Duan C, Sun B, Yang J, Yang S. Multigene editing in the *Escherichia coli* genome via the CRISPR-Cas9 system. *Appl Environ Microbiol.* 2015;81:2506–14.
57. Stemmer M, Thumberger T, del Sol Keyer M, Wittbrodt J, Mateo JL. CCTop: an intuitive, flexible and reliable CRISPR/Cas9 target prediction tool. *PLoS ONE.* 2015;10:e0124633.
58. Zhang H, Cheng Q-X, Liu A-M, Zhao G-P, Wang J. A novel and efficient method for bacteria genome editing employing both CRISPR/Cas9 and an antibiotic resistance cassette. *Front Microbiol.* 2017;8:812.
59. Sharan SK, Thomason LC, Kuznetsov SG, Court DL. Recombinering: a homologous recombination-based method of genetic engineering. *Nat Protoc.* 2009;4:206.
60. DiCarlo JE, Norville JE, Mali P, Rios X, Aach J, Church GM. Genome engineering in *Saccharomyces cerevisiae* using CRISPR-Cas systems. *Nucleic Acids Res.* 2013;41:4336–43.
61. Biot-Pelletier D, Martin VJ. Seamless site-directed mutagenesis of the *Saccharomyces cerevisiae* genome using CRISPR-Cas9. *J Biol Eng.* 2016;10:6.
62. Quan J, Tian J. Circular polymerase extension cloning of complex gene libraries and pathways. *PLoS ONE.* 2009;4:e6441.
63. Gietz RD, Schiestl RH. High-efficiency yeast transformation using the LiAc/SS carrier DNA/PEG method. *Nat Protoc.* 2007;2:31–34.